

Resistive Force theory

The translation of any rigid slender body through a viscous fluid can be analyzed by so-called resistive force theory provided the radius of curvature is large compared with the body radius. To do so we decompose the velocities of each longitudinal element relative to the fluid at infinity into normal and tangential components, U_s and U_n , and similarly decompose the force on that local element into components involving normal and tangential force coefficients as defined in equations (B1c6). The resulting values of C_n and C_s always take the forms of equations (B1d9) and (B1d10), but the coefficients C_1 and C_2 are dependent on the overall geometry of the body (through the integration of stokeslets along the entire axis). For example, a circular ring or torus moving in the direction of one of its major diameters takes values of $C_1 = 0.74$, $C_2 = 0.24$ (R. Johnson and T. Y. Wu, private communication). This is the background for what has come to be known as resistive-force theory in which the force on any element of a slender body such as a cilium or flagellum is calculated from (a) motion of each elemental length of the organelle relative to the fluid at infinity and (b) force coefficients, C_n and C_s , which are determined from the geometry alone. Hancock (1953) and Gray & Hancock (1955) first applied slender-body theory to the analysis of a flagellum along which traveling waves were propagating (Figure 1). The motion of each individual element relative to the

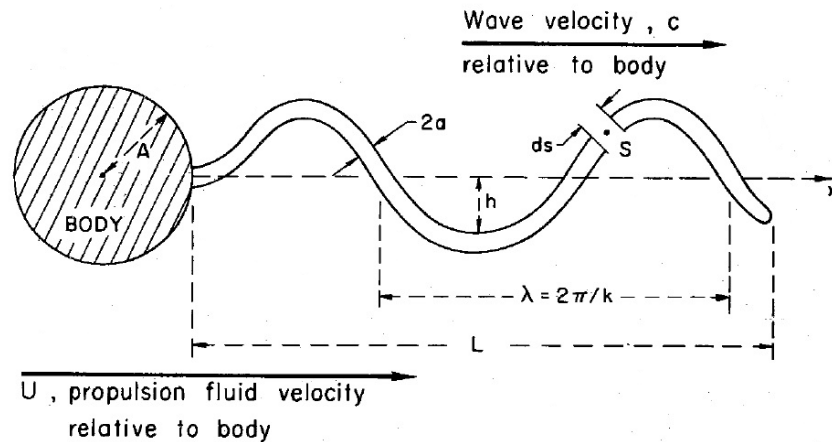


Figure 1: Flagellar propulsion with a planar waveform.

fluid at infinity is thus comprised of a combination of the oscillatory motions due to the passage of the wave and the steady translation of the flagellum through the fluid. The results of Hancock's analyses and the subsequent force coefficients derived by Gray & Hancock (1955) can be interpreted in a simple qualitative way by dividing the axial stokeslet distributions for such a flow into components due to each of these motions and by examining primarily the oscillatory motions for these generally involve larger velocities. It follows that the stokeslet distributions due to the oscillatory motions will be harmonic with distance s from the section at which the integrated velocity is being evaluated (see last section). Lighthill has pointed out that this will result in an integral that will converge more rapidly than those that gave terms like $\ln(s_1 s_2 / a^2)$ in the last section; indeed, the resulting velocity will instead involve a term like $\ln(\lambda/a)$, so that the wavelength, λ , will be the effective body length rather than the overall flagellar length: The resulting force coefficients according to Gray & Hancock (1955) are

$$C_s = \frac{2\pi\mu}{[\ln(2\lambda/a) - 1/2]} \quad (\text{B1e11})$$

$$C_n = 2C_s \quad (\text{Ble12})$$

Moreover Lighthill (1975) showed that the evaluation of the integrals harmonic in s leads to an effective length $\ell^* = 0.09\lambda$, so that

$$C_s = \frac{2\pi\mu}{[\ln(2\ell^*/a) - 0.5]} = \frac{2\pi\mu}{[\ln(2\lambda/a) - 2.90]} \quad (\text{Ble13})$$

$$C_n = \frac{4\pi\mu}{[\ln(2\ell^*/a) + 0.5]} = \frac{4\pi\mu}{[\ln(2\lambda/a) - 1.90]} \quad (\text{Ble14})$$

These can, however, be regarded as only approximate; indeed, it is likely that more accurate coefficients also involve the total flagellar length, L . One indication of this is suggested above, since the stokeslet components due to overall translation of the flagella will contribute terms like $\ln(2L/a)$ as in the case of the translation of rigid slender bodies. We return later to the consequences of such analyses in the context of the fluid mechanics of biological slender bodies. But this section would not be complete without the addition of one other force coefficient, namely that due to rotation at angular velocity Ω of an element of a slender body about its own axis. Chwang & Wu (1974) have shown that the resulting moment M acting on the body about the axis is simply given by

$$M = C_m \Omega ds \quad \text{where} \quad C_m = 4\pi\mu a^2 \quad (\text{Ble15})$$

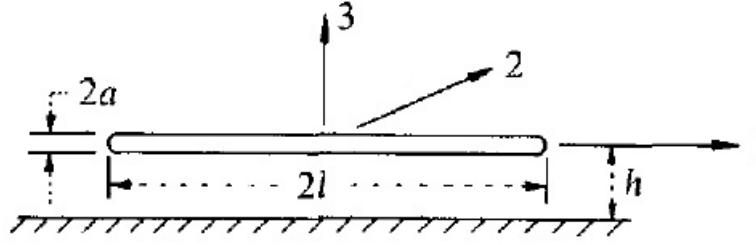
The resistive coefficients on any body are clearly altered by the presence of a nearby boundary. Moreover, there are many situations in microorganism propulsion and in ciliary mechanics in which the slender bodies operate close to solid boundaries. Examples are (a) effects of the presence of the epithelial wall on ciliary dynamics (Blake & Sleight 1974), (b) the motion of spermatozoa, in vivo, either in close proximity to a single wall or within narrow passages, and (c) the effects of a coverslip on studies of microorganism propulsion (Katz 1974 and Winet 1973). Concern about such wall effects has led to a significant number of studies of the influence of nearby boundaries on resistive coefficients for slender bodies.

When the distance of the center of the body from the wall, h , is large compared with its length, 2ℓ , the results of Brenner (1962) for the motion of bodies of arbitrary shape near walls are very useful. Brenner showed that the wall-affected resistive coefficient (drag/ $2\ell U$) denoted by C^* was related to the coefficient, C , in the absence of the boundary by

$$\frac{C^*}{C} = \left[1 - Z \frac{C}{3\pi\mu} \frac{\ell}{h} + O\{(\ell/h)^3\} \right]^{-1} \quad (\text{Ble16})$$

where Z was a function only of the geometry and the direction of particle motion. Examples of the numerical values of Z are (a) $Z = 9/16$ for motion parallel to a single solid plane wall, (b) $Z = 9/8$ for motion perpendicular to a single solid plane wall, (c) $Z = 1.004$ for motion parallel to and equidistant between two solid plane walls, and (d) $Z = 2.1044$ for motion along the axis of a cylindrical tube; other useful values are also given by Brenner (1962). First-order, or $O(\ell/h)$, corrections for wall effects on the resistive coefficients are therefore readily obtained by combination of the equation (Ble16) with the coefficients, such as (Bld9) and (Bld10) in the absence of walls. Some examples are listed in Figure 2, with Cox's coefficients for slender cylindrical bodies (Cox 1970).

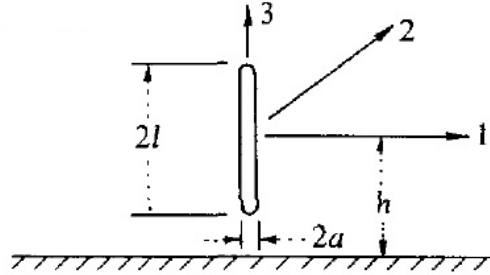
Another general result of particular importance for microorganism propulsion can be deduced from Brenner's result. The value of the ratio $\gamma = C_s/C_n$ for a slender element of a cilium or flagellum is of considerable



$$l/h \ll 1$$

$$l/h \gg 1$$

$$\begin{aligned}
 C_{s1} &= 2\pi\mu \left/ \left[\ln\left(\frac{2l}{a}\right) - 0.807 - \frac{3l}{8h} \right] \right. & C_{s1} &= 2\pi\mu \left/ \left[\ln\left(\frac{2h}{a}\right) \right] \right. \\
 C_{n2} &= 4\pi\mu \left/ \left[\ln\left(\frac{2l}{a}\right) + 0.193 - \frac{3l}{4h} \right] \right. & C_{n2} &= 4\pi\mu \left/ \left[\ln\left(\frac{2h}{a}\right) \right] \right. \\
 C_{n3} &= 4\pi\mu \left/ \left[\ln\left(\frac{2l}{a}\right) + 0.193 - \frac{3l}{2h} \right] \right. & C_{n3} &= 4\pi\mu \left/ \left[\ln\left(\frac{2h}{a}\right) - 1 \right] \right.
 \end{aligned}$$



$$l/h \ll 1$$

$$l/h \rightarrow 1$$

$$\begin{aligned}
 C_{n1} = C_{n2} &= 4\pi\mu \left/ \left[\ln\left(\frac{2l}{a}\right) + 0.193 - \frac{3l}{4h} \right] \right. & C_{n1} = C_{n2} &\rightarrow 4\pi\mu \left/ \left[\ln\left(\frac{2l}{a}\right) - 0.75 \right] \right. \\
 C_{s3} &= 2\pi\mu \left/ \left[\ln\left(\frac{2l}{a}\right) - 0.807 - \frac{3l}{4h} \right] \right. & C_{s3} &\rightarrow 2\pi\mu \left/ \left[\ln\left(\frac{2l}{a}\right) - 1.75 \right] \right.
 \end{aligned}$$

Figure 2: Wall effects on resistive coefficients for the translation of straight slender cylinders with orientation parallel to the wall (upper diagram) and orientation normal to the wall (lower diagram). From Brennen and Winet (1977).

consequence to its propulsive capability. From equation (Ble16) it is seen that the first-order wall effect on this ratio is given by

$$\gamma = \frac{C_s^*}{C_n^*} = \gamma_\infty \left[1 - Z \frac{(C_n^\infty - C_s^\infty) \ell}{3\pi\mu h} \right] \quad (\text{Ble17})$$

where C_n^∞, C_s^∞ are the resistive coefficients in the absence of the wall or walls and $\gamma^\infty = C_s^\infty/C_n^\infty$. Notice in particular that since $C_n^\infty > C_s^\infty$ and provided Z is positive, the effect of the nearby boundary always decreases γ . (Note also from Brenners (1962) quoted values for Z that this quantity is invariably positive for solid boundaries.)

When the slender body is closer to the wall so that ℓ/h is no longer small, the geometry of the body becomes important and a more detailed analysis becomes necessary. Katz & Blake (1975) and Katz, Blake & Payen-Fontana (1975) examined this situation by constructing the flow using a distribution of stokeslets along the axis of slender bodies and satisfying the no-slip condition at the wall or walls by adding the appropriate system of image singularities. The resulting integral equations are solved by the techniques developed by Tillett (1970) and Cox (1970). Solutions were obtained for slender cylinders parallel to a single-plane wall and between two plane walls when the distance, h , from the wall is much smaller than the length, 2ℓ (but still much greater than the radius a). Their results are included in Figure 2; it is significant to note that h now replaces ℓ in the leading term for the coefficient. De Mestre (1973) and de Mestre & Russel (1975) have examined the wall effect for general values of ℓ/h (both large and smaller) and orientations both parallel and perpendicular to the wall. Their results converge asymptotically to the simple results obtained by Brenners relation at small ℓ/h [provided some typo graphical errors in de Mestre & Russel (1975) are corrected] and to the results of Katz, Blake & Payen-Fontana (1975) for parallel slender cylinders. The additional results for perpendicular slender cylinders as $\ell \rightarrow h$ are also incorporated into Figure 2; it is reassuring that if one arbitrarily sets $\ell/h = 1$ in the expressions for $\ell/h \ll 1$, then the result differs only slightly from the more exact expressions for $\ell/h = 1$.